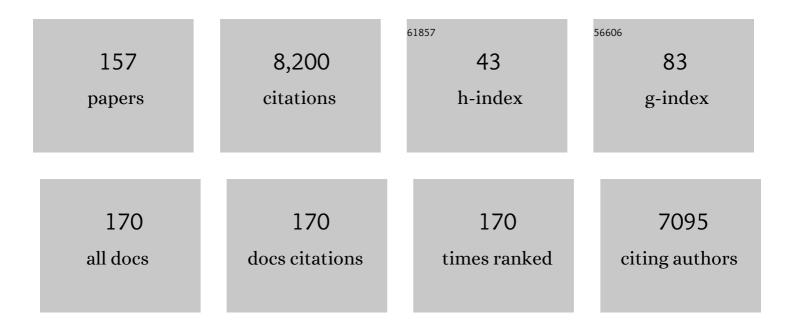
List of Publications by Year in descending order

Source: https://exaly.com/author-pdf/8601487/publications.pdf Version: 2024-02-01



#	Article	IF	CITATIONS
1	Thousands of microbial genomes shed light on interconnected biogeochemical processes in an aquifer system. Nature Communications, 2016, 7, 13219.	5.8	994
2	Measuring Soil Water Content with Ground Penetrating Radar: A Review. Vadose Zone Journal, 2003, 2, 476-491.	1.3	647
3	The emergence of hydrogeophysics for improved understanding of subsurface processes over multiple scales. Water Resources Research, 2015, 51, 3837-3866.	1.7	479
4	Soil moisture content estimation using ground-penetrating radar reflection data. Journal of Hydrology, 2005, 307, 254-269.	2.3	254
5	Estimation of permeable pathways and water content using tomographic radar data. The Leading Edge, 1997, 16, 1623-1630.	0.4	181
6	Measuring Soil Water Content with Ground Penetrating Radar: A Review. Vadose Zone Journal, 2003, 2, 476-491.	1.3	174
7	Effect of Dissolved CO ₂ on a Shallow Groundwater System: A Controlled Release Field Experiment. Environmental Science & Technology, 2013, 47, 298-305.	4.6	168
8	Hydrogeological characterization of the south oyster bacterial transport site using geophysical data. Water Resources Research, 2001, 37, 2431-2456.	1.7	167
9	Estimating the hydraulic conductivity at the south oyster site from geophysical tomographic data using Bayesian Techniques based on the normal linear regression model. Water Resources Research, 2001, 37, 1603-1613.	1.7	144
10	Effects of physical and geochemical heterogeneities on mineral transformation and biomass accumulation during biostimulation experiments at Rifle, Colorado. Journal of Contaminant Hydrology, 2010, 112, 45-63.	1.6	137
11	Hydrogeological parameter estimation using geophysical data: a review of selected techniques. Journal of Contaminant Hydrology, 2000, 45, 3-34.	1.6	132
12	Geophysical Monitoring of Coupled Microbial and Geochemical Processes During Stimulated Subsurface Bioremediation. Environmental Science & amp; Technology, 2009, 43, 6717-6723.	4.6	127
13	Quantifying and relating land-surface and subsurface variability in permafrost environments using LiDAR and surface geophysical datasets. Hydrogeology Journal, 2013, 21, 149-169.	0.9	127
14	Geophysical Imaging of Stimulated Microbial Biomineralization. Environmental Science & Technology, 2005, 39, 7592-7600.	4.6	122
15	The East River, Colorado, Watershed: A Mountainous Community Testbed for Improving Predictive Understanding of Multiscale Hydrological–Biogeochemical Dynamics. Vadose Zone Journal, 2018, 17, 1-25.	1.3	115
16	Landscape topography structures the soil microbiome in arctic polygonal tundra. Nature Communications, 2018, 9, 777.	5.8	105
17	Mineral Transformation and Biomass Accumulation Associated With Uranium Bioremediation at Rifle, Colorado. Environmental Science & Technology, 2009, 43, 5429-5435.	4.6	101
18	Understanding biogeobatteries: Where geophysics meets microbiology. Journal of Geophysical Research, 2010, 115, .	3.3	98

#	Article	IF	CITATIONS
19	Evaluation of infiltration in layered pavements using surface GPR reflection techniques. Journal of Applied Geophysics, 2005, 57, 129-153.	0.9	94
20	Ground-penetrating-radar-assisted saturation and permeability estimation in bimodal systems. Water Resources Research, 1997, 33, 971-990.	1.7	89
21	Low-frequency electrical response to microbial induced sulfide precipitation. Journal of Geophysical Research, 2005, 110, n/a-n/a.	3.3	89
22	A comparison between Gauss-Newton and Markov-chain Monte Carlo–based methods for inverting spectral induced-polarization data for Cole-Cole parameters. Geophysics, 2008, 73, F247-F259.	1.4	88
23	In Situ Long-Term Reductive Bioimmobilization of Cr(VI) in Groundwater Using Hydrogen Release Compound. Environmental Science & Technology, 2008, 42, 8478-8485.	4.6	86
24	Physicochemical Heterogeneity Controls on Uranium Bioreduction Rates at the Field Scale. Environmental Science & Technology, 2011, 45, 9959-9966.	4.6	79
25	Using complex resistivity imaging to infer biogeochemical processes associated with bioremediation of an uranium-contaminated aquifer. Journal of Geophysical Research, 2011, 116, .	3.3	79
26	Joint inversion of crosshole radar and seismic traveltimes acquired at the South Oyster Bacterial Transport Site. Geophysics, 2008, 73, G29-G37.	1.4	78
27	Characterization of Soil Water Content Variability and Soil Texture using GPR Groundwave Techniques. Journal of Environmental and Engineering Geophysics, 2010, 15, 93-110.	1.0	77
28	Mapping the volumetric soil water content of a California vineyard using high-frequency GPR ground wave data. The Leading Edge, 2002, 21, 552-559.	0.4	76
29	Identifying multiscale zonation and assessing the relative importance of polygon geomorphology on carbon fluxes in an Arctic tundra ecosystem. Journal of Geophysical Research G: Biogeosciences, 2015, 120, 788-808.	1.3	74
30	Spatial correlation structure estimation using geophysical and hydrogeological data. Water Resources Research, 1999, 35, 1809-1825.	1.7	72
31	Inversion of tracer test data using tomographic constraints. Water Resources Research, 2006, 42, .	1.7	64
32	Transport and biogeochemical reaction of metals in a physically and chemically heterogeneous aquifer. , 2006, 2, 220.		61
33	Poreâ€scale spectral induced polarization signatures associated with FeS biomineral transformations. Geophysical Research Letters, 2007, 34, .	1.5	59
34	Monitoring CO ₂ Intrusion and Associated Geochemical Transformations in a Shallow Groundwater System Using Complex Electrical Methods. Environmental Science & Technology, 2013, 47, 314-321.	4.6	59
35	Electrical and seismic response of saline permafrost soil during freeze - Thaw transition. Journal of Applied Geophysics, 2017, 146, 16-26.	0.9	59
36	Simulating bioclogging effects on dynamic riverbed permeability and infiltration. Water Resources Research, 2016, 52, 2883-2900.	1.7	57

#	Article	IF	CITATIONS
37	Ferrographic Tracking of Bacterial Transport in the Field at the Narrow Channel Focus Area, Oyster, VA. Environmental Science & Technology, 2001, 35, 182-191.	4.6	56
38	Influence of Hydrological Perturbations and Riverbed Sediment Characteristics on Hyporheic Zone Respiration of CO ₂ and N ₂ . Journal of Geophysical Research G: Biogeosciences, 2018, 123, 902-922.	1.3	56
39	Geophysical monitoring and reactive transport modeling of ureolytically-driven calcium carbonate precipitation. Geochemical Transactions, 2011, 12, 7.	1.8	54
40	Geophysical estimation of shallow permafrost distribution and properties in an ice-wedge polygon-dominated Arctic tundra region. Geophysics, 2016, 81, WA247-WA263.	1.4	54
41	Extrapolating active layer thickness measurements across Arctic polygonal terrain using LiDAR and <i>NDVI</i> data sets. Water Resources Research, 2014, 50, 6339-6357.	1.7	51
42	Spectral induced polarization and electrodic potential monitoring of microbially mediated iron sulfide transformations. Journal of Geophysical Research, 2008, 113, .	3.3	49
43	Introduction to Hydrogeophysics. , 2005, , 3-21.		46
44	A new model for the biodegradation kinetics of oil droplets: application to the Deepwater Horizon oil spill in the Gulf of Mexico. Geochemical Transactions, 2013, 14, 4.	1.8	46
45	Geophysical Monitoring of Hydrological and Biogeochemical Transformations Associated with Cr(VI) Bioremediation. Environmental Science & Technology, 2008, 42, 3757-3765.	4.6	44
46	Microtopographic and depth controls on active layer chemistry in Arctic polygonal ground. Geophysical Research Letters, 2015, 42, 1808-1817.	1.5	44
47	On the complex conductivity signatures of calcite precipitation. Journal of Geophysical Research, 2010, 115, .	3.3	42
48	Coincident aboveground and belowground autonomous monitoring to quantify covariability in permafrost, soil, and vegetation properties in Arctic tundra. Journal of Geophysical Research G: Biogeosciences, 2017, 122, 1321-1342.	1.3	42
49	3D induced-polarization data inversion for complex resistivity. Geophysics, 2011, 76, F157-F171.	1.4	41
50	Electrical Conductivity Imaging of Active Layer and Permafrost in an Arctic Ecosystem, through Advanced Inversion of Electromagnetic Induction Data. Vadose Zone Journal, 2013, 12, 1-19.	1.3	41
51	Riverbed Clogging Associated with a California Riverbank Filtration System: An Assessment of Mechanisms and Monitoring Approaches. Journal of Hydrology, 2015, 529, 1740-1753.	2.3	41
52	Estimation of Soil Hydraulic Parameters in the Field by Integrated Hydrogeophysical Inversion of Time‣apse Groundâ€Penetrating Radar Data. Vadose Zone Journal, 2012, 11, vzj2011.0177.	1.3	40
53	Calibration of a distributed flood forecasting model with input uncertainty using a Bayesian framework. Water Resources Research, 2012, 48, .	1.7	40
54	Advanced Noninvasive Geophysical Monitoring Techniques. Annual Review of Earth and Planetary Sciences, 2007, 35, 653-683.	4.6	39

#	Article	IF	CITATIONS
55	Geochemical characterization using geophysical data and Markov Chain Monte Carlo methods: A case study at the South Oyster bacterial transport site in Virginia. Water Resources Research, 2004, 40, .	1.7	38
56	Reactive facies: An approach for parameterizing fieldâ€scale reactive transport models using geophysical methods. Water Resources Research, 2012, 48, .	1.7	38
57	Factors Governing Sustainable Groundwater Pumping near a River. Ground Water, 2011, 49, 432-444.	0.7	36
58	Reactive Transport Modeling of Induced Selective Plugging by <i>Leuconostoc Mesenteroides</i> in Carbonate Formations. Geomicrobiology Journal, 2013, 30, 813-828.	1.0	36
59	Hierarchical Bayesian method for mapping biogeochemical hot spots using induced polarization imaging. Water Resources Research, 2016, 52, 533-551.	1.7	36
60	Coupled modeling of hydrogeochemical and electrical resistivity data for exploring the impact of recharge on subsurface contamination. Water Resources Research, 2011, 47, .	1.7	35
61	Microbial Metagenomics Reveals Climate-Relevant Subsurface Biogeochemical Processes. Trends in Microbiology, 2016, 24, 600-610.	3.5	35
62	Identifying geochemical hot moments and their controls on a contaminated river floodplain system using wavelet and entropy approaches. Environmental Modelling and Software, 2016, 85, 27-41.	1.9	35
63	Small-scale characterization of vine plant root water uptake via 3-D electrical resistivity tomography and mise-Ã-la-masse method. Hydrology and Earth System Sciences, 2018, 22, 5427-5444.	1.9	35
64	Ground Penetrating Radar in Hydrogeophysics. Vadose Zone Journal, 2008, 7, 137-139.	1.3	34
65	Feedbacks Between Hydrological Heterogeneity and Bioremediation Induced Biogeochemical Transformations. Environmental Science & amp; Technology, 2009, 43, 5197-5204.	4.6	34
66	Bioclogging and Permeability Alteration by <i>L. mesenteroides</i> in a Sandstone Reservoir: A Reactive Transport Modeling Study. Energy & Fuels, 2013, 27, 6538-6551.	2.5	33
67	Identifying key controls on the behavior of an acidic-U(VI) plume in the Savannah River Site using reactive transport modeling. Journal of Contaminant Hydrology, 2013, 151, 34-54.	1.6	33
68	Petrophysical properties of saprolites from the Oak Ridge Integrated Field Research Challenge site, Tennessee. Geophysics, 2013, 78, D21-D40.	1.4	32
69	Sustaining Water Resources: Environmental and Economic Impact. ACS Sustainable Chemistry and Engineering, 2019, 7, 2879-2888.	3.2	32
70	The Snowmelt Niche Differentiates Three Microbial Life Strategies That Influence Soil Nitrogen Availability During and After Winter. Frontiers in Microbiology, 2020, 11, 871.	1.5	32
71	Bayesian hierarchical approach and geophysical data sets for estimation of reactive facies over plume scales. Water Resources Research, 2014, 50, 4564-4584.	1.7	31
72	Predicting sedimentary bedrock subsurface weathering fronts and weathering rates. Scientific Reports, 2019, 9, 17198.	1.6	31

#	Article	IF	CITATIONS
73	Hydrogeophysical investigations of the former S-3 ponds contaminant plumes, Oak Ridge Integrated Field Research Challenge site, Tennessee. Geophysics, 2013, 78, EN29-EN41.	1.4	30
74	Long-term electrical resistivity monitoring of recharge-induced contaminant plume behavior. Journal of Contaminant Hydrology, 2012, 142-143, 33-49.	1.6	29
75	Hysteresis Patterns of Watershed Nitrogen Retention and Loss Over the Past 50Âyears in United States Hydrological Basins. Global Biogeochemical Cycles, 2021, 35, e2020GB006777.	1.9	29
76	Mapping snow depth within a tundra ecosystem using multiscale observations and Bayesian methods. Cryosphere, 2017, 11, 857-875.	1.5	28
77	A distributed temperature profiling method for assessing spatial variability in ground temperatures in a discontinuous permafrost region of Alaska. Cryosphere, 2019, 13, 2853-2867.	1.5	27
78	Time-lapse monitoring of root water uptake using electrical resistivity tomography and mise-Ã-la-masse: a vineyard infiltration experiment. Soil, 2020, 6, 95-114.	2.2	27
79	Depth―and Timeâ€Resolved Distributions of Snowmeltâ€Driven Hillslope Subsurface Flow and Transport and Their Contributions to Surface Waters. Water Resources Research, 2019, 55, 9474-9499.	1.7	25
80	Deep Vadose Zone Respiration Contributions to Carbon Dioxide Fluxes from a Semiarid Floodplain. Vadose Zone Journal, 2016, 15, 1-14.	1.3	24
81	Microbial communities across a hillslopeâ€riparian transect shaped by proximity to the stream, groundwater table, and weathered bedrock. Ecology and Evolution, 2019, 9, 6869-6900.	0.8	24
82	Differential C-Q Analysis: A New Approach to Inferring Lateral Transport and Hydrologic Transients Within Multiple Reaches of a Mountainous Headwater Catchment. Frontiers in Water, 2020, 2, .	1.0	24
83	Emerging technologies and radical collaboration to advance predictive understanding of watershed hydrobiogeochemistry. Hydrological Processes, 2020, 34, 3175-3182.	1.1	24
84	Imaging of plant current pathways for non-invasive root Phenotyping using a newly developed electrical current source density approach. Plant and Soil, 2020, 450, 567-584.	1.8	24
85	Estimating the spatiotemporal distribution of geochemical parameters associated with biostimulation using spectral induced polarization data and hierarchical Bayesian models. Water Resources Research, 2012, 48, .	1.7	23
86	Quantification of Arctic Soil and Permafrost Properties Using Ground-Penetrating Radar and Electrical Resistivity Tomography Datasets. IEEE Journal of Selected Topics in Applied Earth Observations and Remote Sensing, 2017, 10, 4348-4359.	2.3	23
87	Biogenic sulfide control by nitrate and (per)chlorate – A monitoring and modeling investigation. Chemical Geology, 2018, 476, 180-190.	1.4	23
88	Using strontium isotopes to evaluate the spatial variation of groundwater recharge. Science of the Total Environment, 2018, 637-638, 672-685.	3.9	23
89	Investigating Microtopographic and Soil Controls on a Mountainous Meadow Plant Community Using Highâ€Resolution Remote Sensing and Surface Geophysical Data. Journal of Geophysical Research G: Biogeosciences, 2019, 124, 1618-1636.	1.3	23
90	Evaluating temporal controls on greenhouse gas (GHG) fluxes in an Arctic tundra environment: An entropy-based approach. Science of the Total Environment, 2019, 649, 284-299.	3.9	23

#	Article	IF	CITATIONS
91	Joint inversion of geophysical and hydrological data for improved subsurface characterization. The Leading Edge, 2006, 25, 730-734.	0.4	22
92	Time-lapse 3-D electrical resistance tomography inversion for crosswell monitoring of dissolved and supercritical CO2 flow at two field sites: Escatawpa and Cranfield, Mississippi, USA. International Journal of Greenhouse Gas Control, 2016, 49, 297-311.	2.3	22
93	Geophysical Monitoring Shows that Spatial Heterogeneity in Thermohydrological Dynamics Reshapes a Transitional Permafrost System. Geophysical Research Letters, 2021, 48, e2020GL091149.	1.5	22
94	Sulfur Isotopes as Indicators of Amended Bacterial Sulfate Reduction Processes Influencing Field Scale Uranium Bioremediation. Environmental Science & amp; Technology, 2008, 42, 7842-7849.	4.6	21
95	Lessons Learned from Bacterial Transport Research at the South Oyster Site. Ground Water, 2011, 49, 745-763.	0.7	20
96	Assessment of Spatiotemporal Variability of Evapotranspiration and Its Governing Factors in a Mountainous Watershed. Water (Switzerland), 2019, 11, 243.	1.2	20
97	Satellite-derived foresummer drought sensitivity of plant productivity in Rocky Mountain headwater catchments: spatial heterogeneity and geological-geomorphological control. Environmental Research Letters, 2020, 15, 084018.	2.2	20
98	A stateâ€space Bayesian framework for estimating biogeochemical transformations using timeâ€lapse geophysical data. Water Resources Research, 2009, 45, .	1.7	19
99	Stochastic Forward and Inverse Modeling: The "Hydrogeophysical―Challenge. , 2005, , 487-511.		19
100	Watershed zonation through hillslope clustering for tractably quantifying above- and below-ground watershed heterogeneity and functions. Hydrology and Earth System Sciences, 2022, 26, 429-444.	1.9	19
101	On parameterization of the inverse problem for estimating aquifer properties using tracer data. Water Resources Research, 2012, 48, .	1.7	18
102	Remote Monitoring of Freeze–Thaw Transitions in Arctic Soils Using the Complex Resistivity Method. Vadose Zone Journal, 2013, 12, 1-13.	1.3	18
103	Challenges in Building an End-to-End System for Acquisition, Management, and Integration of Diverse Data From Sensor Networks in Watersheds: Lessons From a Mountainous Community Observatory in East River, Colorado. IEEE Access, 2019, 7, 182796-182813.	2.6	18
104	Influence of soil heterogeneity on soybean plant development and crop yield evaluated using time-series of UAV and ground-based geophysical imagery. Scientific Reports, 2021, 11, 7046.	1.6	18
105	Bedrock weathering contributes to subsurface reactive nitrogen and nitrous oxide emissions. Nature Geoscience, 2021, 14, 217-224.	5.4	18
106	HYDROGEOPHYSICAL PARAMETER ESTIMATION APPROACHES FOR FIELD SCALE CHARACTERIZATION. , 2006, , 9-44.		18
107	Stochastic estimation of aquifer geometry using seismic refraction data with borehole depth constraints. Water Resources Research, 2010, 46, .	1.7	16
108	Quantifying shallow subsurface water and heat dynamics using coupled hydrological-thermal-geophysical inversion. Hydrology and Earth System Sciences, 2016, 20, 3477-3491.	1.9	16

#	Article	IF	CITATIONS
109	Galvanic interpretation of selfâ€potential signals associated with microbial sulfateâ€reduction. Journal of Geophysical Research, 2007, 112, .	3.3	15
110	Deep Unsaturated Zone Contributions to Carbon Cycling in Semiarid Environments. Journal of Geophysical Research G: Biogeosciences, 2018, 123, 3045-3054.	1.3	15
111	Estimation of soil classes and their relationship to grapevine vigor in a Bordeaux vineyard: advancing the practical joint use of electromagnetic induction (EMI) and NDVI datasets for precision viticulture. Precision Agriculture, 2021, 22, 1353-1376.	3.1	15
112	Modeling the Impact of Riparian Hollows on River Corridor Nitrogen Exports. Frontiers in Water, 2021, 3, .	1.0	15
113	Paleozoic and Grenvillian Structures in the southern Appalachians: Extended interpretation of seismic reflection data. Tectonics, 1991, 10, 141-170.	1.3	13
114	Geochemical and geophysical responses during the infiltration of fresh water into the contaminated saprolite of the Oak Ridge Integrated Field Research Challenge site, Tennessee. Water Resources Research, 2013, 49, 4952-4970.	1.7	13
115	Commemorating Dr. Gudmundur "Bo―Bodvarsson (1951–2006), a Leader of the Deep Unsaturated Flow and Transport Investigations. Water (Switzerland), 2018, 10, 18.	1.2	13
116	A distributed temperature profiling system for vertically and laterally dense acquisition of soil and snow temperature. Cryosphere, 2022, 16, 719-736.	1.5	13
117	Breakthroughs in field-scale bacterial transport. Eos, 2001, 82, 417-417.	0.1	12
118	Geophysical monitoring and reactive transport simulations of bioclogging processes induced by <i>Leuconostoc mesenteroides</i> . Geophysics, 2014, 79, E61-E73.	1.4	12
119	Coupled land surface–subsurface hydrogeophysical inverse modeling to estimate soil organic carbon content and explore associated hydrological and thermal dynamics in the Arctic tundra. Cryosphere, 2017, 11, 2089-2109.	1.5	12
120	Field-scale estimation of soil properties from spectral induced polarization tomography. Geoderma, 2021, 403, 115380.	2.3	12
121	Surface parameters and bedrock properties covary across a mountainous watershed: Insights from machine learning and geophysics. Science Advances, 2022, 8, eabj2479.	4.7	12
122	From legacy contamination to watershed systems science: a review of scientific insights and technologies developed through DOE-supported research in water and energy security. Environmental Research Letters, 2022, 17, 043004.	2.2	12
123	Data-driven approach to identify field-scale biogeochemical transitions using geochemical and geophysical data and hidden Markov models: Development and application at a uranium-contaminated aquifer. Water Resources Research, 2013, 49, 6412-6424.	1.7	11
124	Meanders as a scaling motif for understanding of floodplain soil microbiome and biogeochemical potential at the watershed scale. Microbiome, 2021, 9, 121.	4.9	11
125	Persistent Source Influences on the Trailing Edge of a Groundwater Plume, and Natural Attenuation Timeframes: The F-Area Savannah River Site. Environmental Science & Technology, 2012, 46, 4490-4497.	4.6	10
126	The Colorado East River Community Observatory Data Collection. Hydrological Processes, 2021, 35, e14243.	1.1	10

#	Article	IF	CITATIONS
127	A deep learning hybrid predictive modeling (HPM) approach for estimating evapotranspiration and ecosystem respiration. Hydrology and Earth System Sciences, 2021, 25, 6041-6066.	1.9	8
128	Electrodic voltages accompanying stimulated bioremediation of a uraniumâ€contaminated aquifer. Journal of Geophysical Research, 2010, 115, .	3.3	7
129	iMatTOUGH: An open-source Matlab-based graphical user interface for pre- and post-processing of TOUGH2 and iTOUGH2 models. Computers and Geosciences, 2016, 89, 132-143.	2.0	7
130	ADVANCED SIMULATION CAPABILITY FOR ENVIRONMENTAL MANAGEMENT (ASCEM): AN OVERVIEW OF INITIAL RESULTS. Technology and Innovation, 2011, 13, 175-199.	0.2	6
131	Geophysical Monitoring of Foam Used to Deliver Remediation Treatments within the Vadose Zone. Vadose Zone Journal, 2012, 11, vzj2011.0160.	1.3	6
132	Visual Data Analysis as an Integral Part of Environmental Management. IEEE Transactions on Visualization and Computer Graphics, 2012, 18, 2088-2094.	2.9	6
133	Depthâ€Resolved Physicochemical Characteristics of Active Layer and Permafrost Soils in an Arctic Polygonal Tundra Region. Journal of Geophysical Research G: Biogeosciences, 2018, 123, 1366-1386.	1.3	6
134	Spatial and temporal variations of thaw layer thickness and its controlling factors identified using time-lapse electrical resistivity tomography and hydro-thermal modeling. Journal of Hydrology, 2018, 561, 751-763.	2.3	6
135	Variability of Snow and Rainfall Partitioning Into Evapotranspiration and Summer Runoff Across Nine Mountainous Catchments. Geophysical Research Letters, 2022, 49, .	1.5	6
136	Introduction to special section on Hydrologic Synthesis. Water Resources Research, 2006, 42, .	1.7	5
137	25. Detecting Perched Water Bodies Using Surface-Seismic Time-Lapse Traveltime Tomography. , 2010, , 415-428.		5
138	Rapidly changing high-latitude seasonality: implications for the 21st century carbon cycle in Alaska. Environmental Research Letters, 2022, 17, 014032.	2.2	5
139	The Relative Importance of Saturated Silica Sand Interfacial and Pore Fluid Geochemistry on the Spectral Induced Polarization Response. Journal of Geophysical Research G: Biogeosciences, 2018, 123, 1702-1718.	1.3	4
140	High-Resolution Spatio-Temporal Estimation of Net Ecosystem Exchange in Ice-Wedge Polygon Tundra Using In Situ Sensors and Remote Sensing Data. Land, 2021, 10, 722.	1.2	4
141	Making a Water Data System Responsive to Information Needs of Decision Makers. Frontiers in Climate, 2021, 3, .	1.3	4
142	BASIN-3D: A brokering framework to integrate diverse environmental data. Computers and Geosciences, 2022, 159, 105024.	2.0	4
143	Integrated imaging of above and below ground properties and their interactions: A case study in East River Watershed, Colorado. , 2018, , .		3
144	Preface to the Special Issue of <i>Vadose Zone Journal</i> on Soil as Complex Systems. Vadose Zone Journal, 2016, 15, 1-3.	1.3	2

#	Article	IF	CITATIONS
145	A hybrid data–model approach to map soil thickness in mountain hillslopes. Earth Surface Dynamics, 2021, 9, 1347-1361.	1.0	2
146	Estimating groundwater dynamics at a Colorado River floodplain site using historical hydrological data and climate information. Water Resources Research, 2016, 52, 1881-1898.	1.7	1
147	Analysis of laboratory data on ultrasonic monitoring of permeability reduction due to biopolymer formation in unconsolidated granular media. Geophysical Prospecting, 2016, 64, 445-455.	1.0	1
148	Estimating active layer, ice-wedge, and permafrost property distributions in Arctic ecosystem using electrical conductivity imaging. , 2013, , .		1
149	Hydrogeological Characterization Using Geophysical Methods. , 2006, , 14-1-14-52.		1
150	Advanced Remedial Methods for Metals and Radionuclides in Vadose Zone Environments. , 2010, , .		0
151	Threeâ€dimensional inversion of EM coupling contaminated spectral induced polarization data. , 2010, , .		0
152	FIELD-SCALE GROUND-PENETRATING-RADAR TOMOGRAPHY AND UNCERTAINTY QUANTIFICATION THROUGH ENTROPY-BASED BAYESIAN INVERSION. , 2013, , .		0
153	Monitoring Arctic landscape variation by pole and kite mounted cameras. Proceedings of SPIE, 2015, , .	0.8	0
154	Remote Sensing to Uav-Based Digital Farmland. , 2018, , .		0
155	Integrated geophysical imaging of permafrost distribution across an Arctic watershed. , 2021, , .		0
156	Longâ€ŧerm timeâ€lapse surface and borehole electrical resistivity monitoring of natural recharge― induced contaminant plume behavior. , 2010, , .		0
157	A Subseasonal Regime Approach for Assessing Intra-annual Variability of Evapotranspiration and Application to the Upper Colorado River Basin. Frontiers in Water, 2022, 3, .	1.0	0